Experimental Mechanics (2023) 63:743–758
https://doi.org/10.1007/s11340-023-00945-y

RESEARCH PAPER

Determination of the Modulus of Elasticity by Bending Tests of Specimens with Nonuniform Cross Section

M. Gebhardt[1,2] · **H. Steinke**[2] · **V. Slowik**[1]

Received: 13 July 2022 / Accepted: 29 January 2023 / Published online: 1 March 2023

Abstract

Background Bending tests offer technical advantages when material testing is performed to determine the modulus of elasticity. In biomechanical studies, beam-like cortical bone specimens subjected to flexural loading are usually characterized by nonuniform cross-sectional properties along the beam axis and a comparatively large spatial variation of the local material properties.

Objective A suitable evaluation method for determining the average modulus of elasticity within the volume of beam-like specimens with nonuniform cross section was to be identified.

Methods A total of 138 samples of human pelvic cortical bone were extracted and tested under flexural loading. Different methods, all based on the linear-elastic flexural theory of beams, were applied to determine the average modulus of elasticity on the basis of measured deformations, and the results were compared. Some of these methods utilized the measured midspan deflection, and others used the elastic curve obtained by digital image correlation.

Results The results showed that it was not appropriate to determine the average modulus of elasticity from only the measured midspan deflection. The consideration of deflections at multiple points along the beam axis is recommended.

Conclusions An evaluation method based on the fitting of the analytically determined elastic curve of the beam with its nonuniform cross-sectional properties to the measured deflections is considered the most appropriate method for determining the average modulus of elasticity of the specimen.

Keywords Modulus of elasticity · Bending test · Biomechanics · Cortical bone · Strain energy · Digital image correlation

Introduction

In medical practice and research, numerical simulations of the mechanical behavior of human organs are of increasing interest; for example, finite element simulations of the buildup of stresses in the human pelvis [1–4]. Reliable experimental identification of relevant material properties is an important precondition to achieve appropriate simulation results. Of predominant importance in this context are the stiffness properties of human tissue, including those of cortical and cancellous bone. Whereas systematic location-dependent stiffness differences should be considered in numerical models to obtain adequate simulation results, random variations may normally be neglected. In many numerical simulation models, human tissues are reproduced by homogeneous components, the effective properties of which need to be determined experimentally, especially those characterizing the material's stiffness. The focus of this paper is on the experimental determination of the modulus of elasticity of human cortical bone. Samples taken from the human lumbo-pelvic system were subjected to flexural loading. Assuming homogeneity of the material, an effective modulus of elasticity was determined on the basis of deformations measured in the bending tests. The obtained results may then be assigned to finite element models for simulating the stress-dependent deformation of the human pelvis. At present, the database of material properties of the

✉ V. Slowik
volker.slowik@htwk-leipzig.de

[1] Institute of Experimental Mechanics, Leipzig University of Applied Sciences, Karl-Liebknecht-Straße 132, 04277 Leipzig, Germany

[2] Institute of Anatomy, Leipzig University, Liebigstraße 13, 04103 Leipzig, Germany

human lumbo-pelvic system appears to be insufficient. One of the goals of this research is to expand this database by applying a reliable testing procedure.

The bending test appears to be a suitable method for testing cortical bone. Direct tension or compression tests are more problematic from the technical point of view because applying a load to the specimen leads to a multiaxial and hard-to-predict state of stress in the vicinity of the specimens' end faces. In the case of tensile tests, this multiaxiality results from lateral clamping forces, and in the case of compression, it results from lateral frictional forces. These problems complicate the determination of the modulus of elasticity characterizing the material's stiffness under a uniaxial state of stress. Theoretically, the influence of the lateral forces at the specimens' end faces vanishes with increasing specimen length, but the maximum size of the bone specimens is commonly limited for anatomical and statistical reasons. The specimens should be small enough to justify the averaging of the local material stiffness. It is undisputed that random variations of the local material properties are larger in biological tissues than in many technical materials. However, if systematic, i.e., anatomically explainable, variations in the stiffness within the specimen are negligible, then the determination of an average modulus of elasticity and the assignment of the value to the corresponding location in a finite element model are justified. In bending tests, this condition can be met because only comparatively small specimen sizes are needed. Another reason for choosing the bending test as the experimental approach is that bone specimens do not necessarily have a straight axis. In direct tension or compression tests, a curved axis leads to significant deviations from the assumed uniform strain distribution in the cross sections of the specimen. However, moderate curvature of beams subjected to bending does not cause significant deviations from basic flexural theory. When the radius of curvature of the beam axis is at least four times the height of the beam, as was the case in the experiments reported here, a straight beam axis may be assumed for the mechanical analysis.

It must be considered that the flexural loading imposed on cortical bone specimens leads to stress concentrations and indentations at the load application point as well as at the supports. However, it is possible to determine the elastic curve of the specimen by measuring the deflection at multiple positions along the beam axis; thus flexural theory can be applied. In this way, the influence of the indentations is eliminated.

A major difference between biological and engineered specimens is the irregularity of the specimen geometry. In the case of the human lumbo-pelvic system, the cross-sectional properties of the beam-like bone specimen may vary markedly along the beam axis mainly due to the natural variation of the cortical layer thickness. When determining the modulus of elasticity on the basis of the measured deformations, it is necessary to consider this variation of the cross-sectional properties and, in this way, to separate its influence from the one of the unavoidable variation of the local material properties. An alternative would be a more invasive processing of the samples to produce strictly rectangular cuboid specimens. However, in this study, the intention was to limit cutting or grinding processes to mitigate their effects on the mechanical behavior of the specimens.

Several investigations involving flexural tests of beam-like cortical bone specimens are reported in the literature. Normally, the determination of the modulus of elasticity is based on the measured midspan deflection of rectangular cuboid beams [5–7]. Lotz et al. [8] tested flat plate cortical bone specimens and determined the modulus of elasticity under consideration of the load point indentation. The consideration of nonuniform cross-sectional properties in flexural tests of beam-like cortical bone specimens has not been reported in the literature before. As far as shear deformation and support indentation in flexural tests are concerned, their effects on the determined moduli of elasticity were extensively studied for other materials. Mujika [9] tested carbon/epoxy composite and Brancheriau et al. [10] wooden samples. It was found in both cases that the before-mentioned influences are not always negligible.

In the "Bending Tests and Deflection Measurements" and "Elastic Curve Determination based on the Optical Displacement Measurement" sections, the applied test setup as well as data acquisition and processing are described. Different evaluation methods for processing the experimental results are presented in the "Methods for Evaluating the Test Results" section, and their suitability is discussed in the "Comparison of the Evaluation Methods" section. It should be noted that the applicability of the evaluation methods proposed in this paper is not limited to the human pelvis or other cortical bone tissue. Possible applications also include naturally grown structural materials. However, the samples of cortical bone from the human lumbo-pelvic complex were a suitable example for the application and comparison of the evaluation methods described here. Due to the natural shape of the pelvis, the samples were characterized by comparatively large variability in thickness and curvature, which made them more realistic than artificially produced samples.

Bending Tests and Deflection Measurements

The specimens of cortical bone were taken from the pelvises of three female and two male human donors. The donors were 76.8 ± 13.4 (53–89) years old. Being part of the body donor program regulated by the Saxonian Death and Funeral Act of 1994 (3rd section, paragraph 18, item 8), the Institute of Anatomy of Leipzig University obtained institutional

approval for the use of postmortem tissues of human body donors. All experiments were performed according to the ethical principles of the Declaration of Helsinki.

Specimen acquisition as well as preparation and storage of the samples were performed according to a standardized procedure proposed by the first author. It was intended to acquire the specimens as less invasive as possible in order to investigate their mechanical properties largely close to nature. The targeted dimensions of the beam-like specimens with intended rectangular cross sections resulted from the geometry of the human pelvis and from the requirements for flexural testing. The selection of the sampling locations was made from an anatomical point of view and by means of computed tomography (CT) scans of the individual donor pelvises. The cortical bone was cut in the deep-frozen state using a diamond thin-cutting band saw, without water cooling. Cancellous bone was removed by sawing and by means of a Stille-Ruskin bone rongeur. For the removal of soft tissue, where possible, served a scalpel. The omission of further post-processing, in particular sawing or grinding on the upper or lower face of the beam-like specimens, resulted in the before-mentioned variation of the cross-sectional properties along the beam axis.

The specimens had approximately rectangular cross sections. The average specimen dimensions were approximately $2.26 \times 9.52 \times 35.4$ mm^3 (height × width × length). The height was the dimension in the loading direction and corresponds to the natural thickness of the cortical bone. A total of 145 samples were successfully harvested, and 138 qualified for inclusion in the examination described below. Reasons for exclusion were strong anatomical abnormality, either geometrical or due to impurity, and, in the case of four samples, failed tests due to accidental dislocation or unacceptable twisting. Table 1 contains information on the variation of the cross-sectional dimensions along the span of the individual specimens as well as within the whole population of all 138 samples. The variation of the height is noticeably greater than that of the width. Graphical representations of the corresponding distributions are shown in the supplementary material.

Figure 1 shows the experimental setup with the loading device made of stainless steel. The circular-cylindrical roller bearings at midspan and at the supports had a diameter 2 mm. The upper roller bearing was rotatable about an axis parallel to the beam axis. Complete design drawings of the experimental setup may be found in the supplementary material.

The simply supported beam-like specimens had a span of 20 mm. During the tests, the periosteum of the cortical bone was directed upward, and its cancellous (inner) side was directed downward. This orientation was chosen to minimize the stiffening effect of residual material adhering to the cortical bone specimen. The remains of the periosteum on the upper side and of the cancellous bone on the lower side have a comparatively small stiffness under compression and tension, respectively. These different behaviors result from the internal structure of the two types of tissue. The periosteum consists mainly of flexible collagen fibers that evade compressive stress. In contrast to that, the cancellous bone has a trabecular structure consisting of small beam-like members with the hollow spaces between them filled with rather liquid bone marrow. In comparison to the cortical bone tested here, the stiffness of cancellous bone is significantly smaller [11]. In addition, the trabecular structure of the latter is damaged in the cutting process, further reducing its tensile stiffness.

At midspan, a transverse force was applied under displacement control by using a 10 kN test frame of an electromechanical testing machine (walter + bai AG - LFEM 600/100/10). A 200 N load cell (Bosche - S40S-G3-0020) served as the force measurement device. The loading velocity was chosen in accordance with a physiologically justifiable strain rate of $\dot{\varepsilon} = 0.005$ s^{-1} [12]. Based on flexural theory, the resulting midspan deflection rate is obtained by $v = \left(\dot{\varepsilon} \cdot l^2\right) / (6 \cdot h)$ for the span l of the beam and the height h at midspan.

The deflection was measured by digital image correlation (DIC) with a Dantec Dynamics Q400 DCM 12.0 (2 × 12 MP sensor, 65 mm focal length, ~100 px/mm resolution, and 4 Hz sampling rate). For evaluating the displacement components, the software Istra4D (version 4.4.7.527) was

Table 1 Variation of the cross-sectional dimensions

Geometrical dimension	Based on the mean values determined for each individual specimen				Difference between maximum and minimum value along the span divided by the corresponding midspan value, determined for each individual specimen			
	Average [mm]	Standard deviation [mm]	Minimum [mm]	Maximum [mm]	Average [%]	Standard deviation [%]	Minimum [%]	Maximum [%]
Height	2.26	0.74	0.94	4.68	40.39	26.35	3.77	185.23
Width	9.52	1.08	6.83	12.29	8.83	6.99	0.49	45.13
Length	35.37	2.79	26.64	39.63	-	-	-	-

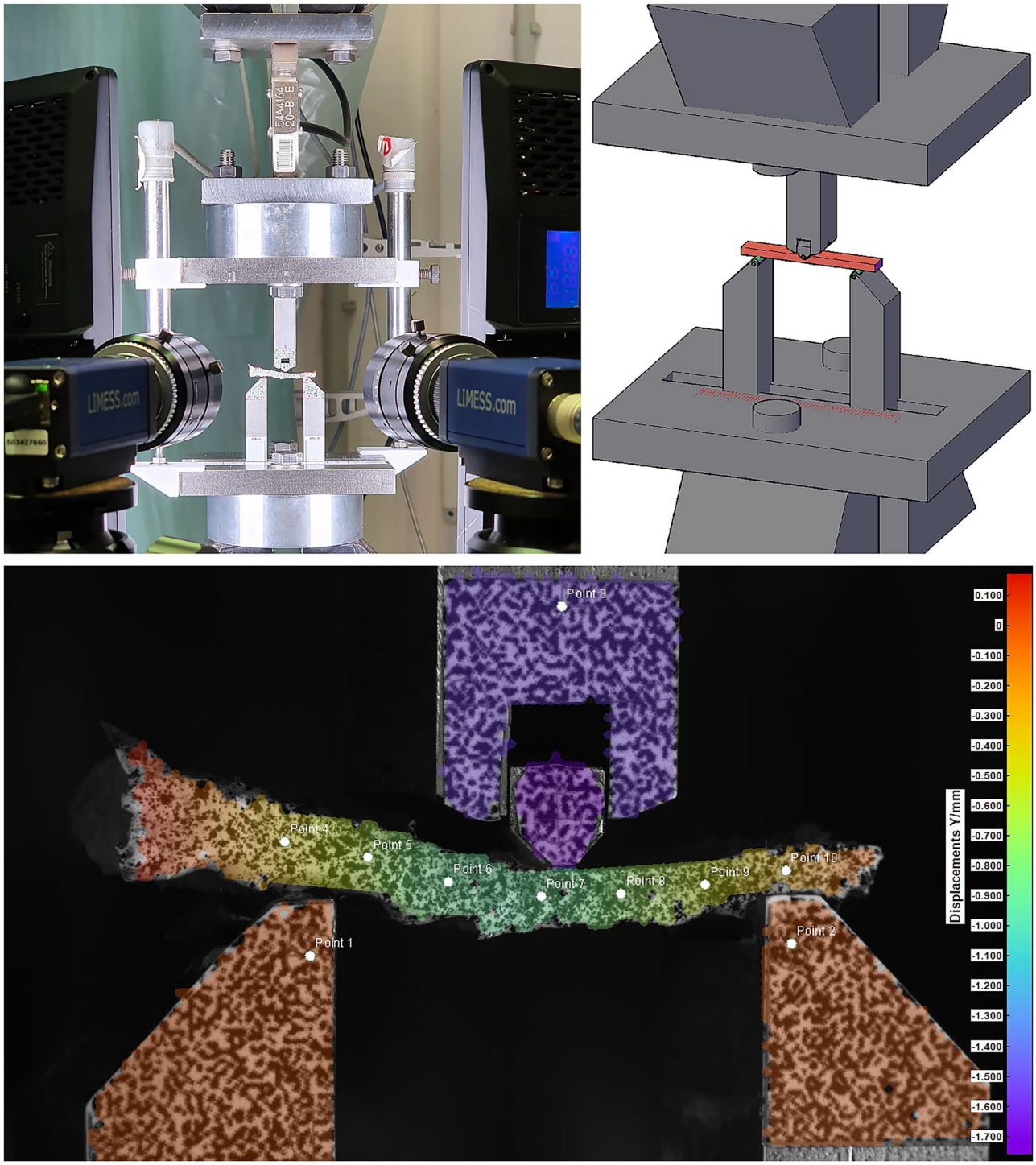

Fig. 1 Experimental setup for the bending tests (top) and full-field map (bottom) of the vertical displacement component obtained by digital image correlation (DIC)

utilized with the grid spacing set to 35 px and the facet size to 39 px. Figure 1 shows in the bottom a full-field map of the vertical displacement component, i.e., of the displacement in the loading direction. The white circles are the evaluation points for the DIC measurement of the 3D coordinates. The intention was to acquire as much information as possible on the deformed state of each specimen.

In addition to the DIC, the load point displacement was measured by linear variable displacement transformers (LVDTs, type W10K from Hottinger Brüel & Kjaer

GmbH) as displacement sensors. The LVDTs were applied to two opposite sides of the loading device, not directly to the specimen. Due to the relatively small compliance of the loading device compared to the specimen deformability, the measured load point displacement may be regarded as the midspan deflection of the beam. However, a portion of the deflection measured in this way results from indentation at the load point and at the supports.

Elastic Curve Determination based on the Optical Displacement Measurement

The 3D displacement components of seven evaluation points on the specimen surface, see Fig. 1 (bottom), were measured by DIC and then projected onto the loading plane. The vertical displacements of these points, i.e., those parallel to the loading direction, are the local deflection values, which were approximated by a continuous function for the elastic curve by conducting a weighted multi-constraint nonlinear least-square fit. The applied constraints are physically justifiable by means of flexural theory and include zero curvature of the elastic curve at the supports and negative curvature along the beam's span. Adequate fits were achieved with a Fourier series having four sine terms and additional linear and constant elements. The applied approximation function and its derivatives are given in equations (1) through (3), which are based on the coordinate system shown in Fig. 2 and contain the Fourier coefficients b_i as well as c and d as additional parameters. The second derivative is zero at the supports, i.e., at $x = x_{\min} = -l/2$ and $x = x_{\max} = +l/2$, thus satisfying the abovementioned zero-curvature constraint.

$$w(x) = \sum_{i=1}^{4}\left(b_i \cdot \sin\left(\frac{i \cdot \pi \cdot (x - x_{\min})}{x_{\max} - x_{\min}}\right)\right) + c \cdot (x - x_{\min}) + d \tag{1}$$

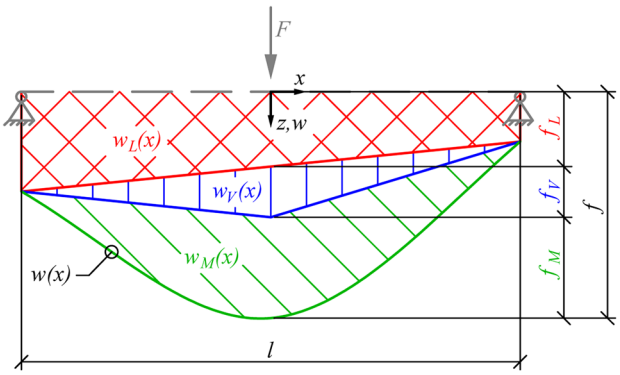

Fig. 2 Contributions to the vertical displacement

$$w'(x) = \left(\frac{\pi}{x_{\max} - x_{\min}}\right) \cdot \sum_{i=1}^{4}\left(i \cdot b_i \cdot \cos\left(\frac{i \cdot \pi \cdot (x - x_{\min})}{x_{\max} - x_{\min}}\right)\right) + c \tag{2}$$

$$w''(x) = -\left(\frac{\pi}{x_{\max} - x_{\min}}\right)^2 \cdot \sum_{i=1}^{4}\left(i^2 \cdot b_i \cdot \sin\left(\frac{i \cdot \pi \cdot (x - x_{\min})}{x_{\max} - x_{\min}}\right)\right) \tag{3}$$

The total lateral (i.e., vertical) displacement $w(x)$, approximating the measured displacement, may be subdivided into different contributions that also influence the modulus of elasticity to be determined. These contributions are schematically represented in Fig. 2 and may be summed according to equation (4).

$$w(x) = w_L(x) + w_V(x) + w_M(x) \tag{4}$$

The contribution of the indentation at the supports $w_L(x)$ is considered by the linear and constant terms in equation (1) and can easily be quantified on the basis of the displacements of the beam axis measured at the supports. By subtracting $w_L(x)$ from the total displacement, the deflection due to the internal forces along the beam's axis is obtained. The deflection $w_V(x)$ due to the shear force is in the case of slender beams significantly smaller than that due to the bending moment $w_M(x)$. Due to the constant shear force in both half-spans, i.e., to the left and right of the load point, the resulting inclination of the beam's axis will also be constant, leading to the bilinear function $w_V(x)$. In flexural theory, the function of the deflection due to the bending moment $w_M(x)$ is commonly referred to as the elastic curve. The corresponding midspan values for the aforementioned three contributions to the total displacement are denoted as f_L, f_V, and f_M (see Fig. 2).

Since the contribution of the shear force is considerably smaller than that of the bending moment, the contribution of the shear force may be estimated under the assumption of uniform cross-sectional properties along the beam axis. Under this simplifying assumption, a theoretical ratio of the midspan displacements, f_V and f_M, i.e., of those due to the shear force and the bending moment, respectively, may be determined. Their theoretical values are

$$f_M = \frac{Fl^3}{48EI} \quad \text{and} \quad f_V = \frac{Fl}{4GA_S} = \frac{Fl(1+\nu)}{2EA_S} \tag{5}$$

where E is the modulus of elasticity, ν is Poisson's ratio, $G = E/(2(1+\nu))$ is the shear modulus, I is the moment of inertia, and A_S is the shear area as a cross-sectional property. Hence,

$$\frac{f_V}{f_M} = \frac{24\, I\, (1+\nu)}{A_S\, l^2} \tag{6}$$

where I and A_S are the average cross-sectional properties along the beam axis. For the rectangular shape of the cross section assumed here (see the "Methods for Evaluating the Test Results" section), the shear area A_S is equal to the total cross-sectional area divided by 1.2. Poisson's ratio ν may be estimated on the basis of uniaxial test results or an assumed value is adopted. This simplification is justifiable because of the non-proportional and, thereby, comparatively small influence of ν, see equations (5) and (6), and also in view of the shear-induced midspan displacement f_V being only a small portion of the total midspan displacement $f_V + f_M$. For the dimensions of the individual specimens tested here, this portion amounts to 4.16% ± 2.61%. Wirtz et al. [11] proposed assuming a value of $\nu = 0.3$ for cortical bone. A reduction of this value by 20% would lead to a reduction of the calculated total midspan displacement $f_V + f_M$ by only about 0.2%.

Using equation (6), we estimated the contribution of the shear deformation to the midspan displacement resulting from the internal forces. The bilinear function of the displacement due to the shear force was then

$$w_V(x) = f_V \cdot \left(1 - \frac{2|x|}{l}\right) \tag{7}$$

The contributions of the shear deformation and of the indentation at the supports may be deducted from the measured total displacements of the beam axis, yielding the displacements resulting from the bending moment only. To obtain a continuous function $w_M(x)$, these modified displacement values along the beam axis were again approximated by a Fourier series but now without additional linear and constant terms because the deflections at the supports are zero.

Methods for Evaluating the Test Results

There are several methods to retrieve an average modulus of elasticity of the material of a beam-shaped specimen. In the following, a total of seven methods, A through G, are presented (see Table 2). Each of these methods includes multiple submethods, which will be explained later. All methods are based on the following assumptions:

- The tested beam is simply supported and subjected to a transverse load at midspan (shown in Fig. 2). Longitudinal frictional forces at the supports may be neglected due to roller bearings. The internal forces may be derived from the external forces by applying equilibrium conditions.
- The cross sections of the beam are rectangular. All external forces act within the plane of symmetry, resulting in so-called symmetric bending.
- The cross-sectional area A and the moment of inertia I about the principal axis normal to the plane of symmetry can vary along the beam's length.
- The span of the beam, i.e., the distance between the supports, is significantly larger than the beam's height, in most cases by a factor of approximately 8, but at least by a factor of 4. Hence, plane sections may be assumed, and Bernoulli's flexural theory may be applied.
- The minimum radius of curvature of the undeformed beam axis is much larger than the beam's height, at least by factor 6. A straight beam axis is assumed and, consequently, the plane section assumption (see above) leads to a linear distribution of the bending strains over the beam's height.
- The deflections measured by DIC at the beam's side face are regarded as those of the beam axis. Anticlastic curvature of the specimen's middle surface due to the Poisson effect is not considered in the evaluation of the measured deflections.
- At least within a certain load range, the beam's deflection is almost proportional to the external force. The material's average modulus of elasticity is determined for a limited load range satisfying this condition and equal under tension and compression.

In view of the particular set of specimens referred to in the present paper, two of the above assumptions require further explanation. First, the midspan curvature of the unloaded specimens was smaller than 0.05 mm^{-1} for more than 95% of all specimens, and the curvature of a circle put through center and supported points of the respective beam axis is even smaller, see distributions in the supplementary material. Consequently, the minimum ratio of the radius of curvature to the average specimen height is larger than about 8. This leads to a deviation of less than 1.5% in the total strain energy of the deflected beam as well as in the calculated midspan deflection. Therefore, the neglect of the curvature is justified for these particular specimens. The strain energy is only slightly underestimated and statistical analyses did not reveal a significant correlation between initial curvature and the determined modulus of elasticity, see Spearman coefficients in the supplementary material. Second, the neglect of the anticlastic curvature on the measured deflections is justified for the present experiments, but is not generalizable. For the present experiments and a Poisson's ratio of 0.3, linear-elastic Finite Element simulations conducted by the authors have shown that the maximum deviation between the deflections in the beam's centerline and at the side faces amounts to less than 3% of the midspan deflection, justifying the neglect of anticlastic curvature. For other specimen geometries and test setups, it might be appropriate to consider both the initial curvature of the beam axis and the anticlastic curvature of the

middle surface. It might also become necessary to consider cross sections the shape of which deviates from the rectangular shape assumed here.

After the flexural load test, the following data were available for further processing:

- The area $A(x)$ and the moment of inertia $I(x)$ of the cross section as dependent on the position x along the beam axis. In the present case, the height and width of the beam were expressed by second-order polynomials that were fitted to values measured at three points along the axis of the respective beam.
- The external force $F(t)$ applied in the experiment as dependent on the time t.
- The midspan deflection $f(t)$ as dependent on the time t as well as the time-dependent elastic curve expressed by multiple deflections at different positions $w(t,x)$. The elastic curve can also be expressed by a fitted continuous function (see the "Elastic Curve Determination based on the Optical Displacement Measurement" section).

Based on these data, the average modulus of elasticity in the axial direction was to be determined. In the beginning, a conventional and simplifying method is presented which is referred to as **Method A** (see Table 2). In addition to the above assumptions, this method is based on a constant moment of inertia I along the beam axis. The external force is related to the midspan deflection. Based on flexural theory, the midspan deflection increment Δf_M is obtained by equation (8).

$$\Delta f_M = \frac{\Delta F\, l^3}{48EI} \tag{8}$$

where ΔF is the force increment, I is the constant moment of inertia and E is the sought-for modulus of elasticity averaged over the entire specimen and the respective force increment. The major disadvantages of Method A are the required assumption of a constant moment of inertia and the falsifying influence of the support indentation. A possible improvement is the evaluation of the beam's midspan curvature increment instead of the midspan deflection increment.

Table 2 Evaluation methods for determining the modulus of elasticity

Method				A							B							C				D							E												F		G			
Short description				Relating midspan deflection to external force							Relating midspan curvature to external force							Equivalence of external and internal work, based on internal forces				Adjusting the calculated elastic curve to measured deflections							Using the local curvature-strain relationship and relating local stress to local strain														Relating local curvature to local bending moment			Equivalence of external and internal work, based on curvature and slope			
Submethod				A0	A2			A4			B1			B2				C2				D1			D2				E4A			E4S			E4M							F4			G3			
				A0Al	A2Al	A2Sl	A2Ml	A4Al	A4Sl	A4Ml	B1Al	B1Sl	B1Ml	B2Al	B2Sl	B2Ml		C2Al	C2Sl	C2Ml	C2Cl	D1Ag	D1Sg	D1Mg	D2Ag	D2Sg	D2Mg		E4Al	E4Ae	E4Ag	E4Sl	E4Se	E4Sg	E4Ml	E4Me	E4Mg				F4Ag	F4Sg	F4Mg	G3Ag	G3Sg	G3Mg	G3Cg
Data used for determining the modulus of elasticity	Conventionally (LVDT) measured midspan displacement		**0**	x																																									
	Based on optically measured displacements	Displacements at multiple measurement points	**1**								x	x	x									x	x	x																						
		Fitted continuous displacement function	**2**		x	x	x							x	x	x		x	x	x	x				x	x	x																				
		Combination of displ. and curvature function	**3**																																											x	x	x	x
		Curvature function (from differentiation)	**4**					x	x	x																			x	x	x	x	x	x	x	x	x				x	x	x				
Elimination of support indentations and shear deformations	None (all influences on the displacement are present)		**A**	x	x			x			x			x				x				x			x				x	x	x										x			x			
	Only indentation eliminated		**S**			x			x			x			x				x				x			x							x	x	x							x			x			
	Indentation and shear deformation eliminated		**M**				x			x			x			x				x				x			x										x	x	x				x			x	
	Indentation eliminated, shear deformation considered		**C**																		x																											x
Evaluation length or position	Midspan position (maximum moment) - local		**l**	x	x	x	x	x	x	x	x	x	x	x	x	x		x	x	x	x								x			x			x							x			x	x	x	x
	Position of maximum strain - local		**e**																											x			x			x												
	Span of the beam or parts of it - global		**g**																			x	x	x	x	x	x			x			x			x							x			x	x	x	x
Remarks				*o*	*o*	*o*	*o*	*o, q*	*o, q*	*o*	*o, p*	*o, p*	*o*	*o, p*	*o, p*	*o*						*t*	*t*	*t*	*t*	*t*	*t*		*q*	*q*	*q, r*	*q*	*q*	*q, r*			*r*				*q, s*	*q, s*	*s*				

o Alternatively to the averaging over multiple load increments, least-square fit of the stress-strain curve; *p* S ≙ A, as the measured sag is independent of the support indentation; *q* S ≙ A, as the curvature is independent of the support indentation; *r* Evaluation is restricted to parts of the beam length where the flexural strain is higher than 50% of the maximum flexural strain

Additional labels for the designation of the submethod: *s* Different evaluation lengths (fu - total span, ha - half span symmetric to midspan, and th - inner third of the span), weighted with the displacement function; *t* Different types of weighting (wt - weighted with the displacement function, uw - unweighting)

This leads to **Method B**. The deflection values at three points in the midspan region of the beam are retrieved from the elastic curve and used for calculating the curvature of the beam axis in this region (shown in Fig. 3). The center point is located at midspan, and the distance between the outer points is l_b. By using this method, the influence of the indentation at the supports is automatically eliminated. It is also possible to eliminate the influence of the shear strain.

Assuming a constant moment of inertia I along the beam axis, the elastic curve $\tilde{w}(x)$ based on the coordinate system in Fig. 3 can be expressed by

$$\tilde{w} = \frac{F}{12EI}x^3 - \frac{Fl}{8EI}x^2 \text{ for } x \geq 0 \tag{9}$$

This leads to

$$s_b = -\tilde{w}\left(x = \frac{l_b}{2}\right) = -\frac{F}{96EI}l_b^3 + \frac{Fl}{32EI}l_b^2 \tag{10}$$

where s_b is the sag of the center point relative to the two outer measurement points (see Fig. 3). In case of an asymmetric elastic curve, the average $\tilde{w}$ value for the two outer measurement points is used. The strain ε_{bottom} at the bottom face with the distance $\tilde{z}_{bottom}$ from the cross section's centroid is

$$\varepsilon_{bottom}(x=0) = -\tilde{w}''(x=0)\cdot\tilde{z}_{bottom} = \frac{Fl\cdot\tilde{z}_{bottom}}{4EI} \text{ with } \tilde{w}''(x=0) = \frac{-Fl}{4EI} \tag{11}$$

Because of the rectangular cross section, $\tilde{z}_{bottom}$ is half of the specimen height. Equations (10) and (11) yield

$$\frac{\varepsilon_{bottom}(x=0)}{s_b} = \frac{24\ l\tilde{z}_{bottom}}{3\ l\cdot l_b^2 - l_b^3} \tag{12}$$

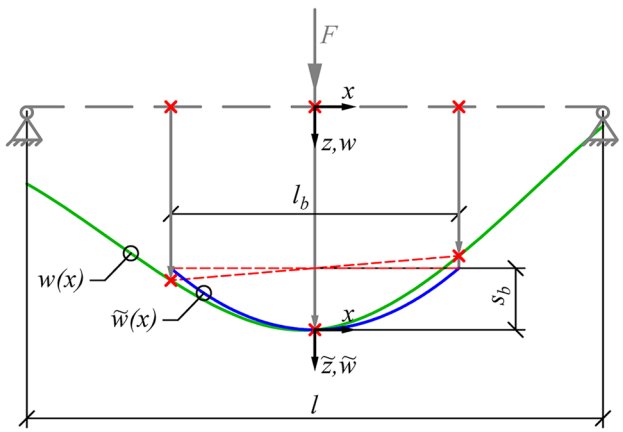

Fig. 3 Curvature measurement over the base length l_b for Method B

For a certain load increment, the average modulus of elasticity can then be calculated by

$$E = \frac{\Delta\sigma_{bottom}(x=0)}{\Delta\varepsilon_{bottom}(x=0)} = \frac{\frac{\Delta Fl}{4I_{midspan}}\cdot\tilde{z}_{bottom}}{\frac{24\ l\tilde{z}_{bottom}}{3\ l\cdot l_b^2 - l_b^3}\cdot\Delta s_b} = \frac{\Delta F}{\Delta s_b}\cdot\frac{3\ l\cdot l_b^2 - l_b^3}{96I_{midspan}} \tag{13}$$

Note that equations (9) through (11) are still based on a constant moment of inertia along the beam axis, although for the stress analysis in equation (13), the one at midspan is used. To consider nonuniform cross-sectional properties, the equivalence between the work W_{ext} done by the external force F and the internal work U done by the internal forces may be used. This approach is here referred to as **Method C**. The external and internal work increments are

$$\Delta W_{ext} = F_0\cdot\Delta f_M + \frac{1}{2}\Delta F\cdot\Delta f_M \tag{14}$$

$$\Delta U = \int_l M_0(x)\cdot\Delta w_M''(x)\,dx + \frac{1}{2}\int_l \Delta M(x)\cdot\Delta w_M''(x)\,dx \tag{15}$$

where M_0 and F_0 are the bending moment and the external force, respectively, at the beginning of the increment. The bending moment M and the resulting deflection w_M are functions of x with values ranging from *-l/2* to *l/2*. Note that for the internal work the absolute values of bending moment and resulting curvature are multiplied. Under the conditions that equilibrium and compatibility are satisfied at the beginning of the load increment and assuming linear-elastic deformation within the increment, it can be stated that

$$F_0\Delta f = \int_l M_0(x)\cdot\Delta w_M''(x)\,dx \tag{16}$$

This leads to

$$\Delta F\cdot\Delta f_M = \int_l \Delta M(x)\cdot\Delta w_M''(x)\,dx = \int_l \frac{\Delta M(x)^2}{EI(x)}dx \text{ with } \Delta w_M''(x) = \frac{\Delta M(x)}{EI(x)} \tag{17}$$

The function of the moment increment $\Delta M(x)$, equation (18), is derived from the equilibrium conditions.

$$\Delta M(x) = \frac{\Delta F}{4}(l - 2|x|) \tag{18}$$

Hence,

$$\Delta f_M = \frac{\Delta F}{16E}\int_l \frac{(l-2|x|)^2}{I(x)}\,dx \tag{19}$$

It is possible to consider the contribution Δf_V of the shear deformation to the midspan displacement increment by adding an extra term to equation (17).

$$\Delta F \cdot \left(\Delta f_M + \Delta f_V\right) = \int_l \frac{\Delta M(x)^2}{EI(x)} dx + \int_l \frac{\Delta V(x)^2}{GA_S(x)} dx \tag{20}$$

where $\Delta V(x)$ is the shear force increment, $A_S(x)$ is the shear area as a cross-sectional property and $G = E/(2(1+\nu))$ is the shear modulus of the material. As stated before, Wirtz et al. [11] proposed adopting a Poisson's ratio of $\nu = 0.3$. An assumption regarding Poisson's ratio is justifiable since its influence is comparatively small. The midspan deflection, including the shear contribution, can be calculated by

$$\begin{aligned} \Delta f_M + \Delta f_V &= \Delta f - \Delta f_L \\ &= \frac{\Delta F}{16E} \int_l \frac{(l - 2|x|)^2}{I(x)}\, dx \\ &\quad + \frac{\Delta F(1+\nu)}{2E} \int_l \frac{1}{A_S(x)}\, dx \end{aligned} \tag{21}$$

where Δf is the total midspan displacement increment, measured or obtained from the fitted displacement function (see the "Elastic Curve Determination based on the Optical Displacement Measurement" section), and Δf_L is the midspan displacement increment resulting from the indentation at the supports (see Fig. 2). The average modulus of elasticity for the load increment is then

$$E = \frac{\Delta F}{\Delta f - \Delta f_L} \cdot \left(\frac{1}{16} \int_l \frac{(l - 2|x|)^2}{I(x)}\, dx + \frac{(1+\nu)}{2} \int_l \frac{1}{A_S(x)}\, dx \right) \tag{22}$$

Method C has a fundamental shortcoming. The evaluation of the experimental results is exclusively based on a single displacement value, the one at midspan. It is expected that the consideration of the entire elastic curve would yield a more reliable value of the average modulus of elasticity. This leads to **Method D,** which is based on the calculation of the theoretical elastic curve and its adjustment to the measured curve. Based on the x, z coordinate system shown in Fig. 2 and on the linearized differential equation of the elastic curve, equation (23), the solution presented in equation (24) is derived for the present problem.

$$w_M''(x) = \frac{-M(x)}{EI(x)} \tag{23}$$

$$\begin{aligned} &w_M(x) = w_M(0) + w_M'(0) \cdot x - \int_0^x \int_0^{\hat{x}} \frac{M(\tilde{x})}{EI(\tilde{x})} d\tilde{x} d\hat{x} \quad \text{with} \\ &M(\tilde{x}) = \frac{F}{4}\left(l - 2|\tilde{x}|\right) \end{aligned} \tag{24}$$

The continuity conditions at midspan are automatically satisfied, and the boundary conditions

$$w_M\left(-l/2\right) = w_M\left(l/2\right) = 0 \tag{25}$$

at the supports lead to

$$\begin{aligned} &\begin{Bmatrix} w_M(0) \\ w_M'(0) \end{Bmatrix} = \begin{bmatrix} 1 & -l/2 \\ 1 & l/2 \end{bmatrix}^{-1} \cdot \frac{F}{E} \cdot \begin{Bmatrix} \Omega(-l/2) \\ \Omega(l/2) \end{Bmatrix} \quad \text{with} \\ &\Omega(x) = \int_0^x \int_0^{\hat{x}} \frac{l - 2|\tilde{x}|}{4I(\tilde{x})} d\tilde{x} d\hat{x} \end{aligned} \tag{26}$$

allowing the determination of the midspan deflection $w_M(0) = f_M$ and corresponding slope $w_M'(0)$. Then, using equation (24), the deflection at an arbitrary point x can be calculated and adjusted to the measured values by varying the modulus of elasticity. For a single deflection increment Δw_M at position x resulting from the force increment ΔF, this adjustment leads to

$$E = \frac{\Delta F}{\Delta w_M(x)} \cdot \left(\left(\frac{x}{l} + \frac{1}{2}\right)\Omega\left(l/2\right) - \left(\frac{x}{l} - \frac{1}{2}\right)\Omega\left(-l/2\right) - \Omega(x) \right) \tag{27}$$

The moduli of elasticity obtained for different positions x are averaged over the beam's span. In some submethods, a weighted average is calculated. When determining $w_M(x)$, the influences of the indentation at the supports and of the shear deformation may be eliminated, as stated above.

All evaluation methods described thus far are based on displacement values, either directly on the locally measured values or on those calculated from a fitted continuous displacement function. An alternative approach is to differentiate the fitted continuous displacement function twice and to use the obtained curvature $w_M''(x)$ for further data processing. In **Method E**, an axial strain increment at a certain position x and at a certain distance z from the cross section's centroid is determined according to Bernoulli flexural theory by

$$\Delta\varepsilon(x,z) = -\Delta w_M''(x) \cdot z \tag{28}$$

The modulus of elasticity in the cross section at position x and within the considered load increment is then obtained by

$$E = \frac{\Delta\sigma(x,z)}{\Delta\varepsilon(x,z)} \text{ with } \Delta\sigma(x,z) = \frac{\Delta M(x)}{I(x)} \cdot z \tag{29}$$

The position x may be at midspan or at the strain maximum. It is also possible to average over an evaluation length l_e according to equation (30). The corresponding submethods (see Table 2) are explained below.

$$E = \frac{1}{l_e} \int_{l_e} \frac{\Delta\sigma(x,z)}{\Delta\varepsilon(x,z)} dx \tag{30}$$

Method F is also based on the evaluation of the curvature, i.e., of the second derivative of the elastic curve. However, instead of relating a stress increment to a strain increment, the differential equation of the elastic curve, equation (23), is directly applied to relate a curvature increment $\Delta w''_M(x)$ to a bending moment increment $\Delta M(x)$. Within the load increment concerned, the modulus of elasticity averaged over an evaluation length l_e is obtained by

$$E = \frac{1}{l_e}\int_{l_e} \frac{-\Delta M(x)}{\Delta w''_M(x)\cdot I(x)}dx \text{ with } \Delta M(x) = \frac{\Delta F}{4}(l - 2|x|) \tag{31}$$

The evaluation length l_e may be the total span of the beam or only an inner part of it, symmetric with respect to midspan. In the latter case, perturbations from the low-curvature regions close to the supports may be eliminated.

Method G utilizes the equivalence between the external and internal work, as in Method C. However, the internal work U is calculated on the basis of the curvature and slope of the elastic curve rather than on the basis of the internal forces. Equivalent to equation (20), the following equation describes the equivalence between the external and internal work. The second term on the left-hand side contains the contribution of the shear deformation.

$$\begin{aligned}\Delta F \cdot \left(\Delta f_M + \Delta f_V\right) = &\int_l \Delta M(x)\cdot \Delta w''_M(x)dx \\ &+ \int_l \Delta V(x)\cdot \Delta w'_V(x)dx\end{aligned} \tag{32}$$

Replacing the internal forces by derivatives of the elastic curve using

$$\begin{aligned}&\Delta M(x) = \Delta w''_M(x)\cdot EI(x) \text{ and} \\ &\Delta V(x) = \Delta w'_V(x)\cdot GA_s(x) = \Delta w'_V(x)\cdot \frac{E}{2(1+\nu)}A_s(x)\end{aligned} \tag{33}$$

yields the following expression of the average modulus of elasticity within the considered load increment.

$$E = \frac{\Delta F \cdot \left(\Delta f_M + \Delta f_V\right)}{\int_l \left(\Delta w''_M(x)\right)^2 \cdot I(x)\,dx + \frac{1}{2(1+\nu)}\int_l \left(\Delta w'_V(x)\right)^2 \cdot A_s(x)\,dx} \tag{34}$$

In curvature-based methods, the indentation at the supports theoretically does not influence the determined modulus of elasticity. It must be considered, however, that the continuous displacement function to be differentiated twice is just an approximation. It is therefore advisable to deduct the contribution of the indentation, in some sub-methods also the contribution of the shear force, from the displacement function prior to differentiation and further processing, as explained in the "Elastic Curve Determination based on the Optical Displacement Measurement" section.

Table 2 gives an overview of the seven evaluation methods (A through G) and their submethods. For systematization and comprehensibility, all submethods are labeled by a combination of four characters, such as "A0Al". The first letter indicates one of the seven evaluation methods, i.e., Method A through Method G. In the second position, the number ("0" through "4") specifies the type of data used for retrieving the modulus of elasticity (see Table 2 for definitions). The fitting of a continuous function to the measured displacements (indicated by "2" in the second position) and the differentiation for obtaining a curvature function (indicated by "4" in the second position) are explained in the "Elastic Curve Determination based on the Optical Displacement Measurement" section. The number "3" in the second position applies only to Method G. There, the fitted displacement function is used for retrieving its midspan value, whereas the internal work is determined on the basis of the curvature and slope functions. In submethods A4**, the midspan strain is calculated from the midspan curvature (where "*" represents any character).

The character in the third position ("A", "S", "M", or "C") describes which influences on the displacements have been deducted from the measured values (see the "Elastic Curve Determination based on the Optical Displacement Measurement" section). In the case of "A", "S", and "M" in the third position, the displacement function, obtained after the corresponding type of elimination, is regarded as resulting from the bending moment only. Although this is incorrect for "A" (no falsifying influences eliminated) and "S" (only support indentation eliminated), the evaluation results may serve for comparisons of the individual evaluation methods (see the "Elimination of Falsifying Influences" section). The character "C" in the third position is used when the shear deformation is directly considered in the expression for the internal mechanical work, rather than by deducting its contribution from the displacement function, as done in the case of "M".

The character at the fourth position ("l", "e", or "g") specifies which part of the beam's span is considered for retrieving the modulus of elasticity. In the case of "l" at the fourth position, only values acquired at midspan are used, i.e., at the position of maximum moment, and in the case of "e" at the position of maximum strain. The character "g" is used when input data along the total span of the beam or, in the case of Methods E and F, along a portion of the span are evaluated. The corresponding options for the evaluation length are expressed by the Suffixes "fu", "ha", or "th" (see footnotes in Table 2). In Methods D through G, the evaluation length was always equal to the

total span. In Method F, the displacement function served as a weighting function for averaging along the evaluation length, whereas in Method D, two different types of weighting were applied (see Suffixes "wt" and "uw" specified in the footnotes of Table 2).

The range of the stress-strain curve used for the evaluation of the modulus of elasticity has also been varied (see first footnote in Table 2). Within this evaluation range, averaging over multiple load increments or, alternatively, fitting a straight line to the load–displacement curve was conducted. More explanation may be found in the "Evaluation Range of the Stress-Strain Curve" section.

Comparison of the Evaluation Methods

Suitability Criteria for the Evaluation Methods and Plausibility Checks

The chosen approach for assessing the suitability of the individual evaluation methods includes statistical analyses and plausibility checks. For the present experimental investigations, there are no reference values to serve as the basis of comparison for the measured moduli of elasticity. This makes it difficult to identify the most suitable evaluation method. It should also be noted that, in the present case, the 138 individual samples were extracted from different locations of the human pelvises of multiple donors. This means that the samples do not necessarily belong to a common base population. Nevertheless, coefficients of variation (*CV*s) as well as different types of relative deviation (*D*) were calculated and are discussed below. These values are independent of the mean values and characterize the variation in the determined modulus of elasticity. In order to separate the effects of the evaluation method from those of material inhomogeneity and cross-sectional nonuniformity, the influences of analysis assumptions, see Table 2, were first quantified for each individual specimen, i.e., on the specimen level, and later statistically evaluated for the entire population of tested specimens. Regarding the coefficient of variation of the modulus of elasticity of all samples ($CV_{pop,E}$), it is assumed for simplicity that all samples belong to the same base population and consist of the same material. After the elimination of falsifying influences, the evaluation methods yielding smaller values of $CV_{pop,E}$ are considered to provide more reliable results than those yielding larger $CV_{pop,E}$ values.

In addition to statistical parameters, other indicators for the suitability of the different evaluation methods were also applied, and plausibility checks were conducted. The latter included rank correlation analyses according to Spearman. This nonparametric methodology was chosen because the considered variables are not necessarily normally distributed. A correlation coefficient of 1 indicates the strongest positive correlation and of -1 indicates the strongest negative correlation. A first plausibility check by means of Spearman correlation analyses revealed deviating evaluation results when method F with full determination length was applied, i.e., the submethods F4*gfu. For all other methods, there is a strong positive correlation between the modulus of elasticity and the material strength (with an average correlation coefficient of 0.9). Less pronounced is the correlation with the apparent density (average of 0.4) and with the strain at ultimate stress (average of -0.6). The abovementioned submethods F4*gfu do not exhibit these correlations. Furthermore, they also show a significantly larger variation than the other methods. This may be attributed to the curvature-based determination of the local modulus of elasticity and its averaging over the entire span of the beam. The curvature function being the second derivative of the elastic curve, i.e., of the fitted displacement function, fluctuates more strongly than the displacement function itself. In extreme cases, even sign changes of the curvature may be observed near the supports, resulting in singularities of the locally determined modulus of elasticity. This adverse characteristic of the F4*gfu submethods could not be compensated for even by weighting the displacement function. Consequently, the F4*gfu submethods were excluded from the following comparisons.

Correlation plots and additional results of Spearman correlation analyses may be found in the supplementary material.

Evaluation Range of the Stress-Strain Curve

To determine the modulus of elasticity, it is essential to specify a certain part of the ascending stress-strain curve, the slope of which yields the sought-for elastic property. Normally, the slope within a fixed stress range, i.e., between fixed stress limits relative to the peak value, is evaluated. The intention is to limit the determination of the modulus of elasticity to a section of the stress-strain curve with a characteristic and fairly constant slope. Since the variance of the mechanical properties of the cortical bone samples tested here was comparatively high, the evaluation of the slope within a flexible range rather than within a fixed range of the stress-strain curve was deemed appropriate. For this purpose, a modification of Keuerleber's approach [13] was utilized. It is based on the assumption that the slope maximum represents the "true" modulus of elasticity, which is free of disturbing influences if the test is conducted properly. To obtain more representative results, a range of the stress-strain curve limited by 75% of the maximum slope was used for the determination of the modulus of elasticity rather than the maximum slope as a single value. The evaluation range specified in this way was searched within the

ascending branch of the stress-strain curve between 15 and 100% of the ultimate stress. This type of evaluation range (referred to hereafter as the refined evaluation range) proved to be the most favorable in this study. It must be noted that the abovementioned slope is represented by consecutive difference quotients of the stress-strain curve consisting of discrete measurement steps. The corresponding procedure is in the following referred to as incremental determination.

For comparison, a fixed evaluation range was also considered. It was comparatively short and limited by 25% and 50% of the ultimate stress. Within the refined range as well as within the fixed range, the modulus of elasticity was determined for discrete stress increments and subsequently averaged over the respective evaluation range. The scatter of the modulus of elasticity within the evaluation range may be characterized by the coefficient of variation $CV_{er,E}$, and the difference between the fixed and refined evaluation ranges can be quantified by the relative deviation $D_{CV_{er,E},fixed-refined} = \left(CV_{er,E,fixed} - CV_{er,E,refined}\right)/CV_{er,E,refined}$. After excluding statistical outliers on the specimen level by applying the 1.5-interquartile-range rule, the average over all evaluation methods amounts to $\overline{D}_{CV_{er,E},fixed-refined} = -7.57\ \%$ with a standard deviation of $\pm 5.13\ \%$. The corresponding values without exclusion of outliers are $8.80\ \% \pm 19.67\ \%$. This shows that a smaller variation within the evaluation range can be achieved mainly by excluding outliers. Considering that the refined range is significantly larger than the fixed range, a reduced variation may also result from the refinement. The necessity of excluding outliers is also seen when the obtained values of the moduli of elasticity are compared. On average, over all evaluation methods, there is a relative deviation $D_{E,fixed-refined} = \left(E_{fixed} - E_{refined}\right)/E_{refined}$ of $\overline{D}_{E,fixed-refined} = 2267\ \% \pm 15446\ \%$ without the exclusion of outliers and of $-2.49\ \% \pm 1.58\ \%$ with the exclusion of the same, i.e., almost no deviation. Figure 4 shows the relative deviation between the moduli of elasticity obtained for the two different evaluation ranges. The confidence intervals (black lines with caps) presented in Figs. 4 through 8 were determined by bootstrapping for a confidence level of 95%.

For the less complex evaluation methods, in particular for Methods A and B, the slope of the stress-strain curve was alternatively determined by least-squares fitting of a straight line to the measured values (see also the first footnote in Table 2). The average coefficients of determination are $R_{er,E,fixed} = 99.41\ \% \pm 2.33\ \%$ for the fixed evaluation range and $R_{er,E,refined} = 99.48\ \% \pm 2.38\ \%$ for the refined evaluation range. The relative deviations of the moduli of elasticity obtained by least-square fitting from the incrementally determined ones $D_{E,lsq-inc} = \left(E_{lsq} - E_{inc}\right)/E_{inc}$ are on average $-1.80\ \% \pm 0.83\ \%$ and $-1.51\ \% \pm 1.26\ \%$ for the fixed and refined evaluation ranges, respectively. The individual deviations for the different evaluation methods are presented in Fig. 5. Because of their small values, it is concluded that the incremental determination over the refined evaluation range with subsequent averaging and exclusion of statistical outliers provides sufficient accuracy. Therefore, only moduli of elasticity obtained by this procedure are discussed below.

Elimination of Falsifying Influences

A reliable determination of the modulus of elasticity requires the elimination of falsifying influences if they have a significant impact on the results. It was found that the indentation at the supports has the greatest impact. As expected, there is no difference between the submethods with (**S*) and without (**A*) elimination of the support indentation provided that the evaluation of the modulus of elasticity is based on the curvature of the displacement function, as is the case for the submethods *4**. Due to the differentiation, the linear and constant components of the displacement function and consequently the contribution of the support indentation disappear. The same holds true for Method B. Although based on measured deflections, this method effectively evaluates the midspan curvature. These findings are demonstrated in the lower part of Fig. 6 by showing the relative deviation

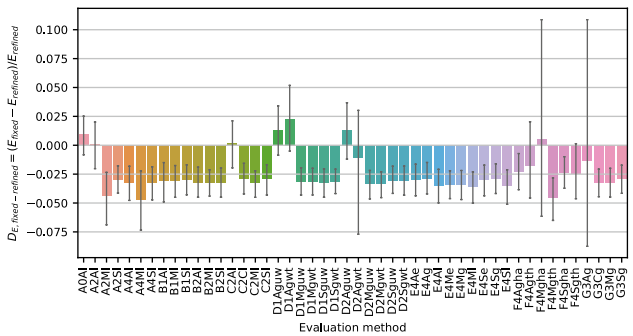

Fig. 4 Relative deviation between the moduli of elasticity determined for the refined and fixed evaluation range, incremental determination and averaging over the evaluation range with the exclusion of statistical outliers, confidence intervals determined by bootstrapping for a confidence level of 95%

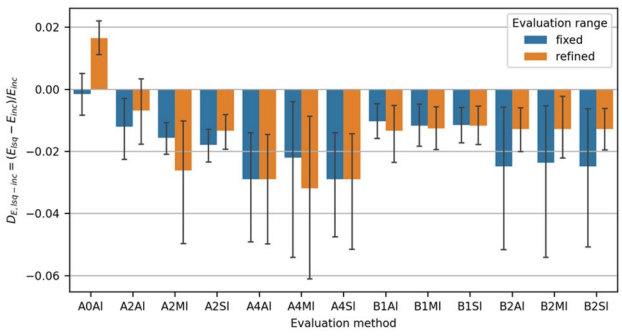

Fig. 5 Relative deviation between the moduli of elasticity determined incrementally and by means of least-squares fitting, confidence intervals determined by bootstrapping for a confidence level of 95%

$D_{E,S-A} = \left(E_S - E_A\right)/E_A$ of the moduli of elasticity obtained by submethods eliminating support indentations only (**S*) from those obtained by submethods without any elimination of falsifying influences (**A*). Averaged over all submethods except B*** and *4**, the relative deviation $\overline{D}_{E,S-A}$ amounts to 83.8 % ± 18.5 %, meaning that a significantly higher modulus of elasticity is obtained when the support indentation is eliminated. For evaluation method G, however, the relative deviation is negative, which is in contrast to the other methods. This can be explained by the underlying calculation according to equation (34), which relates midspan deflection to curvature. This ratio is greater with than without support indentation.

The upper part of Fig. 6 shows the Spearman coefficients for the correlation between $D_{E,S-A}$ and different contributing factors. As expected for the submethods with large $D_{E,S-A}$ (i.e., A2**, C***, and D***), the correlation to the measured support indentation is the strongest. The larger the support indentation, especially in the elastic range, the higher the relative deviation between the moduli of elasticity.

The effect of the elimination of shear deformation, in addition to the elimination of support indentation, is presented in Fig. 7. The lower part of the figure shows the relative deviation $D_{E,M-S} = \left(E_M - E_S\right)/E_S$ of the moduli of elasticity determined with elimination of the shear deformation (**M*) from those determined without it (**S*). The upper part of Fig. 7 shows the Spearman coefficients for the correlation between $D_{E,M-S}$ and different contributing factors. As expected from the theory of elasticity, there is a significant correlation with the average beam height. The other correlations are not as strong. It can also be noted that submethods based on measured displacements or fitted displacement functions exhibit a considerably narrower confidence interval for $D_{E,M-S}$ than curvature-based methods, especially Method D. The same observation is made when comparing the submethods based on a global evaluation (***g) to those based on a local evaluation. One reason for this difference is that the local determination does not compensate for fluctuations in the displacement values measured along the beam axis. Moreover, in the case of a nonuniform cross section, the evaluated location does not necessarily coincide with the location of the stress or strain maximum. It must also be considered that, in general, the differentiation of the displacement function leads to a "loosening" of the relationship to the measured displacements. This may reduce the evaluation reliability for the modulus of elasticity in the case of a curvature-based evaluation.

Based on the observed confidence intervals, also shown in Fig. 7, Methods B, C, D, and G appear to be suitable evaluation methods yielding plausible results. The relative deviation due to the elimination of the shear influence amounts to $\overline{D}_{E,M-S} = 4.99\ \% \pm 2.52\ \%$ averaged over the four abovementioned evaluation methods. Although this effect is much smaller than that of the support indentation, the relative deviation may reach up to 20% in the case of a specimen with a large height-to-span ratio. For the methods that allow a direct consideration of the shear deformation, namely, Methods C and G, there was no significant effect of the elimination of the shear deformation. For these methods, the relative deviation $D_{E,C-M} = \left(E_C - E_M\right)/E_M$ amounts to, on average, $\overline{D}_{E,C-M} = -1.71\ \% \pm 3.27\ \%$.

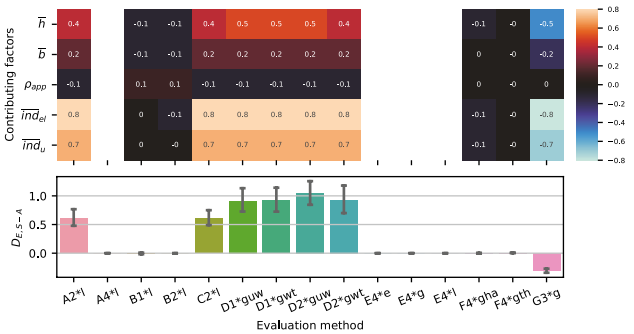

Fig. 6 Bottom: Relative deviation between the moduli of elasticity determined without (**A*) and with (**S*) elimination of the support indentation, confidence intervals determined by bootstrapping for a confidence level of 95%; Top: Spearman correlation coefficients for chosen contributing factors ($\overline{h}$, average height of the beam; $\overline{b}$, average width of the beam; ρ_{app}, apparent density; $\overline{ind}_{el}$, average support indentation at elastic limit; and $\overline{ind}_u$, average support indentation at peak load)

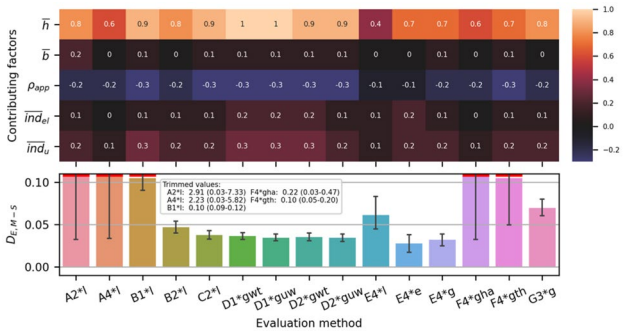

Fig. 7 Bottom: Relative deviation between the moduli of elasticity determined without (**S*) and with (**M*) elimination of the shear deformation, with support indentation eliminated in both cases. The bars with the red top line were trimmed for clarity. Confidence intervals were determined by bootstrapping for a confidence level of 95%. Top: Spearman correlation coefficients for chosen contributing factors ($\overline{h}$, average height of the beam; $\overline{b}$, average width of the beam; ρ_{app}, apparent density; $\overline{ind}_{el}$, average support indentation at elastic limit; and $\overline{ind}_u$, average support indentation at peak load)

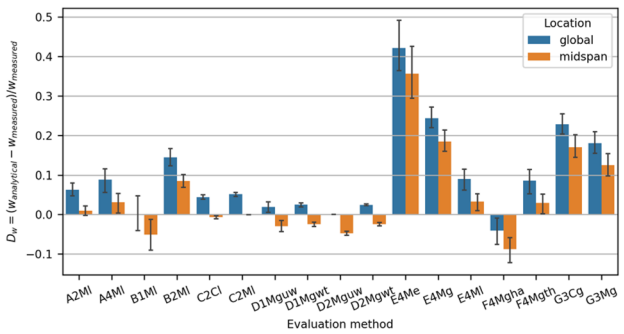

Fig. 8 Relative deviation of the analytical elastic curve from the measured curve, where the analytical elastic curve was calculated for the modulus of elasticity obtained by different evaluation methods; confidence intervals determined by bootstrapping for a confidence level of 95%

Forward Analysis of the Elastic Curve

For each of the evaluation methods, the obtained modulus of elasticity was used to calculate the theoretical elastic curve for the simply supported and centrically loaded beam with nonuniform cross-sectional properties. This analytically obtained elastic curve was then compared with the one fitted to the measured displacements. Support indentation and shear deformation were eliminated from the fitting function, hereafter referred to as the measured elastic curve. Figure 8 shows the relative deviations between the analytical and measured elastic curves for the evaluation methods eliminating all falsifying influences (**M*) or correctly considering the shear deformation (**C*). The smallest deviations occur with evaluation methods C and D, which indicates the good suitability of these methods. As expected, there is no deviation for evaluation method C2Ml at midspan and for D2Mguw over the entire span (labeled "global" in Fig. 8). This is because the evaluation method D2Mguw utilizes the same theoretical elastic curve as the forward analysis, and the evaluation method D is a global extension of C.

It should be noted that the fitting function used for the elastic curve (see the "Elastic Curve Determination based on the Optical Displacement Measurement" section) differs from the physically correct function for the simply supported and centrically loaded beam with a uniform cross section. The theoretically correct function consists of two third-order polynomials that coincide at midspan. However, using such fitting functions would require more measurement points along the beam axis, and the fitting would be more difficult. But possibly, some of the problems that occur when curvature-based evaluation methods are applied could be solved in this way. This may be the subject of a future study based on the present experimental data.

Observations Regarding the Entire Population of the Tested Specimens

As discussed in the "Suitability Criteria for the Evaluation Methods and Plausibility Checks" section, the individual specimens do not necessarily belong to a common base population. They originate from different donors and different locations within the pelvis. Despite these differences, and because it was attempted to extract comparable specimens from the cortical bone, the coefficient of variation $CV_{pop,E}$ of the modulus of elasticity over the entire population of tested specimens is regarded as an additional indicator for the evaluation quality. Since the comparison of these coefficients is reasonable only in the case of complete elimination of falsifying influences, it is limited to the submethods satisfying this condition. Table 3 contains the corresponding coefficients of variation listed in ascending order.

Method D exhibits the lowest coefficient of variation. This is another indication of the good suitability of this method. The average modulus of elasticity determined by Method D2Mgwt amounts to 1748 MPa with a confidence interval from 1511 to 1971 MPa determined by bootstrapping for a confidence level of 95%. For comparison, by the conventional evaluation method (i.e., submethod A0Al), which is based on the midspan deflection measurement, a modulus of elasticity of 882 MPa was obtained with a confidence interval from 753 to 1006 MPa. The corresponding coefficient of variation $CV_{pop,E}$ amounts to only approximately 0.885. However, the modulus of elasticity obtained in this way is unrealistic. Expectedly, the material stiffness is underestimated, mainly due to support indentations. For further evaluation methods, the determined moduli of elasticity and associated statistical results can be found in the supplementary material.

Table 3 Coefficients of variation for all specimens and the different submethods

Method	**D1Mguw**	**D2Mguw**	**D2Mgwt**	**D1Mgwt**	**C2Ml**	**F4Mgth**	**G3Mg**	**E4Mg**
$CV_{pop,E}$	0.823	0.824	0.829	0.830	0.834	0.846	0.858	0.861
Method	**B2Ml**	**B1Ml**	**E4Ml**	**E4Me**	**F4Mgha**	**F4Mgfu**	**A4Ml**	**A2Ml**
$CV_{pop,E}$	0.862	0.866	0.882	0.920	1.306	2.038	6.554	7.186

Verification Tests on Synthetic Materials

In order to prove the reliability of the proposed evaluation methods, comparative tests of specimens made of homogeneous materials were conducted. Two beam-like specimens with the dimensions $2 \times 8 \times 36$ mm^3 (height × width × length) were made of polymethyl methacrylate (PMMA) by sawing and five specimens of different shape, see Fig. 9, were made of polylactic acid (PLA) by Fused Deposition Modeling.

All seven specimens were tested in its original orientation and, in addition, in an upside-down orientation. Information on the specimen preparation and test procedure as well as the complete results may be found in the supplementary material. The four tests of the PMMA beams yielded a modulus of elasticity of 3663 MPa ± 31 MPa (mean value ± standard deviation) by using the preferred evaluation method (Method D2Mgwt) and 3501 MPa ± 27 MPa by conventual midspan deflection-based determination (Method A0Al). These measured moduli of elasticity are slightly above the range of 3000 MPa to 3400 MPa reported for PMMA in the literature [14]. This may be attributed to aging effects and varying test methods. Turning over the beams had almost no influence (mean absolute deviation less than 1%). The modulus of elasticity of PLA varies normally in a wider range due to the strong dependence on the manufacturing process. For the PLA specimens, 3485 MPa ± 50 MPa were obtained by Method D2Mgwt and 3200 MPa ± 133 MPa conventionally by Method A0Al. As stated before, Method A0Al tends to underestimate the material stiffness. The moduli of elasticity determined for the PLA specimens with nonuniform cross sections, see Fig. 9, has a mean absolute deviation from the one obtained for the specimen with uniform cross section by only 1.39% when the preferred Method D2Mgwt is applied. Apparently, the nonuniformity is appropriately considered by the evaluation method and has almost no effect on the final result. The above mean absolute deviation amounts to 4.63% in case a conventional evaluation by Method A0Al is conducted. As far as the differences between the evaluation methods are concerned, the observations made for the cortical bone specimens could be confirmed. If all falsifying influences are eliminated, i.e., the support indentation and the shear deformation, the recommended Methods C and D yield almost the same moduli of elasticity. The latter have a mean absolute deviation from the value obtained by the preferred Method D2Mgwt of less than 2.2%.

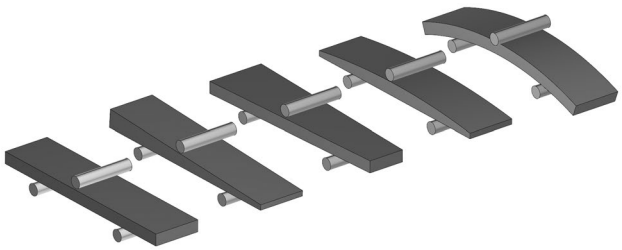

Fig. 9 Shapes of the specimens made of Polylactic acid (PLA) for the verification tests (schematically shown); length of the specimens 36 mm; from left to right: uniform rectangular cross section with the reference dimensions 2×8 mm^2 (height × width); linearly varying height, at the supports 2.6 mm and 1.4 mm; linearly varying width, at the supports 9 mm and 7 mm; quadratic parabola for the height, 1.8 mm at the supports and 2.2 mm at midspan; curved beam with uniform cross section (reference dimensions), constant radius of curvature 50.5 mm

Conclusions

It is possible to determine the modulus of elasticity of beam-like specimens with a nonuniform cross section by means of three-point bending tests and appropriate evaluation methods. It is strongly recommended to eliminate the falsifying influence of the support indentation from the results. This requires the measurement of the beam's displacement at multiple points along its axis, not only at midspan.

In this study, several evaluation methods proved to be suitable for retrieving the average modulus of elasticity of the material from measured displacements. However, Method D is considered the most appropriate. It is based on the fitting of the elastic curve analytically determined by definite integrals to the measured deflections. In comparative evaluations of the experimental results, Method D proved to be less sensitive than the other methods to changes in the evaluation procedure. Neither the type of database, in particular the measurement point displacements (submethods D1**) or a fitted displacement function (submethods D2**), nor the weighting of the displacements had a substantial influence on the obtained modulus of elasticity. It is recommended, however, to use a fitted displacement function for the calculation since the influence of local fluctuations of the measured values is reduced in this way. In addition, measurement points located outside the beam's span may also be used for the curve fitting.

As stated previously, the elimination of falsifying influences is critical, especially the elimination of support indentations. In this study, the proposed evaluation method yielded on average a 109.9% higher modulus of elasticity than the conventional determination, i.e., determination exclusively based on the midspan displacement (submethod A0Al).

Method C is also attractive for practical applications, in particular submethods C2Ml and C2Cl, which eliminate falsifying influences. It involves much less computational effort and leads to comparable results. This may be because

the deflection maximum is, in most cases, not far off midspan, even for beams with a nonuniform cross section. Variation of the cross-sectional properties along the beam's axis is also considered in Method C.

The evaluation method D2Mgwt was successfully used to determine the modulus of elasticity of human pelvic cortical bone. The complete results and their correlation with harvesting locations as well as with donor-specific and other data will be presented in a forthcoming publication.

Supplementary Information The online version contains supplementary material available at https://doi.org/10.1007/s11340-023-00945-y.

Acknowledgements We extend special thanks to Dr.-Ing. Thomas Klink from Leipzig University of Applied Sciences and Dipl.-Ing. Sascha Kurz from Leipzig University for their support and contributions to the experimental work.

Author Contribution Marc Gebhardt: Conceptualization, Methodology, Software, Validation, Formal analysis, Investigation, Resources, Data Curation, Writing - Original Draft, Writing - Review & Editing, Visualization, Project administration, Funding acquisition; Hanno Steinke: Investigation, Resources, Writing - Review & Editing, Supervision; Volker Slowik: Conceptualization, Methodology, Investigation, Resources, Writing - Original Draft, Writing - Review & Editing, Supervision, Project administration, Funding acquisition.

Funding Open Access funding enabled and organized by Projekt DEAL. We acknowledge support from the German Federal Ministry for Economic Affairs and Energy (Zentrales Innovationsprogramm Mittelstand, Reference number ZIM 16KN051655) and the Saxonian State Ministry for Higher Education, Research and the Arts (Stipend reference number 31004 70 809). The sponsors played no role in the study design, data collection, data analysis, data interpretation, or writing of the manuscript.

Data Availability The data that supports the findings of this study is available from the corresponding author upon reasonable request.

Declarations

Conflict of Interests The authors declare no known competing financial interests or personal relationships that could have appeared to influence the work presented in this paper.

References

1. Anderson AE, Peters CL, Tuttle BD, Weiss JA (2005) Subject-specific finite element model of the pelvis: development, validation and sensitivity studies. J Biomech Eng 127(3):364–373. https://doi.org/10.1115/1.1894148
2. Dalstra M, Huiskes R, van Erning L (1995) Development and validation of a three-dimensional finite element model of the pelvic bone. J Biomech Eng 117(3):272–278. https://doi.org/10.1115/1.2794181
3. Qu A, Wang D, Zeng X, Wang Q (2018) Dynamic response and material sensitivity analysis of pelvic complex numerical model under side impact. Biomed Mater Eng 29(4):499–512. https://doi.org/10.3233/BME-181005
4. Ravera EP, Crespo MJ, Catalfamo Formento PA (2018) A subject-specific integrative biomechanical framework of the pelvis for gait analysis. Proc Inst Mech Eng H J Eng Med 232(11):1083–1097. https://doi.org/10.1177/0954411918803125
5. Albert CI, Jameson J, Harris G (2013) Design and validation of bending test method for characterization of miniature pediatric cortical bone specimens. Proc Inst Mech Eng H 227(2):105–113. https://doi.org/10.1177/0954411912463868
6. Mick E, Steinke H, Wolfskämpf T, Wieding J, Hammer N, Schulze M, Souffrant R, Bader R (2015) Influence of short-term fixation with mixed formalin or ethanol solution on the mechanical properties of human cortical bone. Curr Dir Biomed Eng 1(1):335–339. https://doi.org/10.1515/cdbme-2015-0083
7. Wieding J, Mick E, Wree A, Bader R (2015) Influence of three different preservative techniques on the mechanical properties of the ovine cortical bone. Acta Bioeng Biomech 17(1):137–146. https://doi.org/10.5277/ABB-00067-2014-03
8. Lotz JC, Gerhart TN, Hayes WC (1991) Mechanical properties of metaphyseal bone in the proximal femur. J Biomech 24(5):317–329. https://doi.org/10.1016/0021-9290(91)90350-V
9. Mujika F (2007) On the effect of shear and local deformation in three-point bending tests. Polym Test 26(7):869–877. https://doi.org/10.1016/j.polymertesting.2007.06.002
10. Brancheriau L, Bailleres H, Guitard D (2002) Comparison between modulus of elasticity values calculated using 3 and 4 point bending tests on wooden samples. Wood Sci Technol 36(5):367–383. https://doi.org/10.1007/s00226-002-0147-3
11. Wirtz DC, Schiffers N, Pandorf T, Radermacher K, Weichert D, Forst R (2000) Critical evaluation of known bone material properties to realize anisotropic FE-simulation of the proximal femur. J Biomech 33(10):1325–1330. https://doi.org/10.1016/S0021-9290(00)00069-5
12. Richard HA, Kullmer G, Nöcker D (2013) Biomechanik. Grundlagen und Anwendungen auf den menschlichen Bewegungsapparat. Springer Vieweg, Wiesbaden (ISBN: 978-3-8348-0384-9)
13. Keuerleber M (2006) Bestimmung des Elastizitätsmoduls von Kunststoffen bei hohen Dehnraten am Beispiel von PP. Universität Stuttgart, Germany (Dissertation)
14. Rösler J (2007) Mechanical behaviour of engineering materials: Metals, ceramics, polymers, and composites. Springer, Berlin, Heidelberg (ISBN: 978-3-540-73446-8)